

ORIGINAL ARTICLE

# Strong EGFR signaling in cell line models of ERBB2-amplified breast cancer attenuates response towards ERBB2-targeting drugs

F Henjes<sup>1</sup>, C Bender<sup>1</sup>, S von der Heyde<sup>2</sup>, L Braun<sup>3</sup>, HA Mannsperger<sup>1</sup>, C Schmidt<sup>1</sup>, S Wiemann<sup>1</sup>, M Hasmann<sup>4</sup>, S Aulmann<sup>3</sup>, T Beissbarth<sup>2</sup> and U Korf<sup>1</sup>

Increasing the efficacy of targeted cancer therapies requires the identification of robust biomarkers suitable for patient stratification. This study focused on the identification of molecular mechanisms causing resistance against the anti-ERBB2-directed therapeutic antibodies trastuzumab and pertuzumab presently used to treat patients with ERBB2-amplified breast cancer. Immunohistochemistry and clinical data were evaluated and yielded evidence for the existence of ERBB2-amplified breast cancer with high-level epidermal growth-factor receptor (EGFR) expression as a separate tumor entity. Because the proto-oncogene EGFR tightly interacts with ERBB2 on the protein level, the hypothesis that high-level EGFR expression might contribute to resistance against ERBB2-directed therapies was experimentally validated. SKBR3 and HCC1954 cells were chosen as model systems of EGFR-high/ERBB2-amplified breast cancer and exposed to trastuzumab, pertuzumab and erlotinib, respectively, and in combination. Drug impact was quantified in cell viability assays and on the proteomic level using reverse-phase protein arrays. Phosphoprotein dynamics revealed a significant downregulation of AKT signaling after exposure to trastuzumab, pertuzumab or a coapplication of both antibodies in SKBR3 cells but no concomitant impact on ERK1/2, RB or RPS6 phosphorylation. On the other hand, signaling was fully downregulated in SKBR3 cells after coinhibition of EGFR and ERBB2. Inhibitory effects in HCC1954 cells were driven by erlotinib alone, and a significant upregulation of RPS6 and RB phosphorylation was observed after coincubation with pertuzumab and trastuzumab. In summary, proteomic data suggest that high-level expression of EGFR in ERBB2-amplified breast cancer cells attenuates the effect of anti-ERBB2-directed antibodies. In conclusion, EGFR expression may serve as diagnostic and predictive biomarker to advance personalized treatment concepts of patients with ERBB2-amplified breast cancer.

*Oncogenesis* (2012) 1, e16; doi:10.1038/oncsis.2012.16; published online 2 July 2012

**Subject Categories:** Mode of action of cancer therapeutics

**Keywords:** EGFR; ERBB2; HER2; erlotinib; trastuzumab; pertuzumab

## INTRODUCTION

The family of epidermal growth-factor receptors (EGFRs) consists of four members: EGFR, ERBB2 (HER2), ERBB3 and ERBB4. Overexpression of the orphan receptor ERBB2 was found in 20–25% of breast tumors and has been associated with poor prognosis and short overall survival of breast cancer patients.<sup>1</sup> Ligand-activated ERBB family members preferentially dimerize with ERBB2,<sup>2</sup> which prolongs the internalization rate of ERBB2-containing heterodimers<sup>3</sup> resulting in amplified, sustained and prolonged signaling.<sup>4,5</sup> Accordingly, ERBB2 has long been recognized as a promising therapeutic target. Trastuzumab, a humanized monoclonal antibody,<sup>6</sup> was approved by the Food and Drug Administration in 1998 as the first therapeutic antibody to treat patients with ERBB2-amplified metastatic breast cancer and is today mostly used in combination with conventional chemotherapeutics.<sup>7</sup> Clinical trials have demonstrated a significant benefit of trastuzumab for various adjuvant treatment regimens of early non-metastasized breast cancer.<sup>8</sup> The molecular basis underlying the clinical efficacy of trastuzumab is multifaceted and different mechanisms are involved.<sup>9,10–13</sup> For example, trastuzumab has been reported to disrupt ligand-independent ERBB2/ERBB3 heterodimer formation in ERBB2-overexpressing

cells, thus leading to ERBB3 inactivation.<sup>14</sup> The ERBB2-targeting antibody pertuzumab was tailored to prevent heterodimerization of ERBB2 with ligand-activated ERBB receptors.<sup>15</sup> Thus, a combined application of trastuzumab and pertuzumab should cause an immediate disruption of ERBB2-containing dimers and inhibit a dimerization of ERBB2 with ligand-activated receptors. The therapeutic efficacy of trastuzumab and pertuzumab as combinatorial treatment was explored in mouse xenograft models of ERBB2-positive breast cancer, and the results demonstrated a strongly enhanced antitumor activity compared with single-drug treatments.<sup>16</sup> Ongoing clinical trials assess the benefit of trastuzumab plus pertuzumab as the standard therapy for ERBB2-amplified human breast cancer.<sup>17,18</sup> However, *de novo* resistance against trastuzumab and/or pertuzumab was reported for various cell line models of human ERBB2-amplified breast cancer,<sup>19–21</sup> and the elucidation of resistance mechanisms might result in the identification of biomarkers for further clinical validation. A likely target is EGFR, a well-known proto-oncogene,<sup>22</sup> because this receptor is stabilized by ERBB2 on the protein level as revealed by combinatorial small interfering RNA strategies.<sup>21</sup> Small-molecule drugs, such as erlotinib, target the EGFR kinase domain and prevent signal propagation in a ligand-

<sup>1</sup>Division of Molecular Genome Analysis, German Cancer Research Center (DKFZ), Heidelberg, Germany; <sup>2</sup>Department of Medical Statistics, University Medical Center Göttingen, Göttingen, Germany; <sup>3</sup>Institute of Pathology, Heidelberg University, Heidelberg, Germany and <sup>4</sup>Pharma Research and Early Development (pRED), Roche Diagnostics GmbH, Penzberg, Germany. Correspondence: Dr U Korf, Division of Molecular Genome Analysis, German Cancer Research Center (DKFZ), Im Neuenheimer Feld 580, D-69120 Heidelberg, Germany.

E-mail: u.korf@dkfz.de

Received 26 March 2012; revised 4 May 2012; accepted 7 May 2012

independent way. Erlotinib has been approved for the treatment of locally advanced or metastatic non-small cell lung cancer and, in combination with gemcitabine, for locally advanced and unresectable or metastatic pancreatic cancer.<sup>23</sup> Therefore, targeting EGFR in addition to ERBB2 might be an efficient strategy for ERBB2-amplified tumors that additionally express EGFR. Recently, ERBB2-amplified breast cancer with high-level phosphorylation of EGFR was, based on its poor clinical outcome, suggested to represent a separate molecular entity.<sup>24</sup> Besides that, case studies on a coapplication of trastuzumab and anti-EGFR drugs, for example, gefitinib, demonstrated clinical benefit in ERBB2-positive breast cancer of patients whose tumors stained positive for EGFR.<sup>25</sup>

Both receptors, EGFR and ERBB2, activate MAPK as well as PI3K/AKT signaling cascades. Although EGFR mainly activates MAPK signaling, ERBB2 phosphorylation stimulates both the pathways.<sup>26,27</sup> ERBB3 was identified as a kinase-defective receptor and therefore requires cross-activation by other ERBB family members as prerequisite for a potent initiation of PI3K/AKT signaling.<sup>28,29</sup> Thus, EGFR/ERBB2 dimers can induce phosphorylation of AKT, although less efficiently compared with ERBB2/ERBB3 complexes.<sup>30</sup> Signals from both the pathways, PI3K/AKT and MAPK, merge on the level of the protein kinase p70S6K, which controls cellular protein synthesis via phosphorylation of RPS6. In addition, activated p70S6K exerts a direct negative feedback on receptor tyrosine kinase signaling via inhibition of IRS1.<sup>31</sup>

This study aimed to evaluate the benefit of anti-EGFR inhibitors in cell line models of ERBB2-amplified breast cancer with *de novo* resistance against trastuzumab and/or pertuzumab<sup>19,20,32</sup> by measuring ERK1/2 and AKT phosphorylation rates as central players of fast downstream signaling.<sup>33,34</sup> To assess the impact of drug on cell growth and proliferation, dynamics of RPS6 and RB phosphorylation was additionally monitored. Reverse-phase protein arrays (RPPA) with near-infrared fluorescent readout were used to obtain quantitative proteomic data.<sup>35</sup> To ascertain clinical significance of this study, tumor samples were analyzed by immunohistochemistry for coexpression of EGFR in ERBB2-positive breast cancer specimens.

## RESULTS

Validation of SKBR3 and HCC1954 cells as model systems of EGFR-high/ERBB2-amplified human breast cancer

Cell lines such as SKBR3 and HCC1954, both with amplified ERBB2 and high abundance of EGFR, represent well-accepted model systems of ERBB2-positive breast cancer. Western blot analysis and quantitative PCR data confirmed a high-level expression of EGFR and ERBB2 and revealed that ERBB3 is of higher abundance in

SKBR3 cells, whereas HCC1954 cells produce the receptor tyrosine kinase c-MET (Supplementary Figure S1B). ERBB4 expression was very low at the transcript level and not detectable by western blot in either cell line (data not shown). ERK1/2 and AKT were present in comparable amounts in both cell lines, whereas a much stronger expression of RPS6 was seen in SKBR3 cells (Supplementary Figure S1C). The phosphorylation rate of ERK1/2 in SKBR3 cells did not change upon starvation in line with other results (Supplementary Figure S1D).<sup>36</sup> Starvation reduced the phosphorylation rate of ERK1/2 in HCC1954 cells, AKT in SKBR3 cells and RPS6 in both cell lines (Supplementary Figure S1D). Furthermore, in HCC1954 cells, the phosphorylation status of AKT increased after serum starvation, which was also observed in a previous study (Supplementary Figure S1D).<sup>37</sup>

Targeting of EGFR reduces cell viability in cell line models of EGFR-high/ERBB2-amplified breast cancer

Viability assays were carried out in both cell lines to assess the impact of single drugs as well as combinatorial drug treatments. Trastuzumab and pertuzumab, applied alone or in combination over a treatment period of 96 h, did not significantly change the viability of HCC1954 cells, identifying these cells as resistant towards treatment with anti-ERBB2 antibodies. Erlotinib, added alone or in combination with other compounds, significantly reduced the viability of HCC1954 cells (Figure 1a). Incubation of SKBR3 cells for 96 h with erlotinib and trastuzumab reduced the fraction of viable cells by 20% and 45%, respectively (Figure 1b). An even stronger impact on SKBR3 cell viability, a decrease by 60%, was seen when erlotinib and trastuzumab were applied in combination implying an additive drug effect (Figure 1b). In contrast, only marginal influence on cellular viability of SKBR3 cells was seen after exposure to pertuzumab, confirming SKBR3 cells as pertuzumab-resistant (Figure 1b)<sup>38</sup>.

Trastuzumab and pertuzumab downregulate AKT but not ERK1/2 signaling in cell line models of EGFR-high/ERBB2-amplified breast cancer

Next, the impact of drugs on EGF-induced signaling was analyzed on the phosphoproteomic level. First of all, addition of EGF to SKBR3 cells induced a fast phosphorylation of ERK1/2 and AKT with a maximum of activation after 12 min and an elevated state of AKT phosphorylation persisting for at least 60 min (Figures 2a and b). Preincubation of SKBR3 cells with trastuzumab significantly reduced the AKT baseline phosphorylation of time point 0 min ( $P < 0.05$ ), which was not seen after pretreatment with pertuzumab (Figure 2b). On the other hand, pertuzumab reduced the first peak of AKT phosphorylation observable 12 min after EGF addition but not so trastuzumab (Figure 2b). However, notable differences

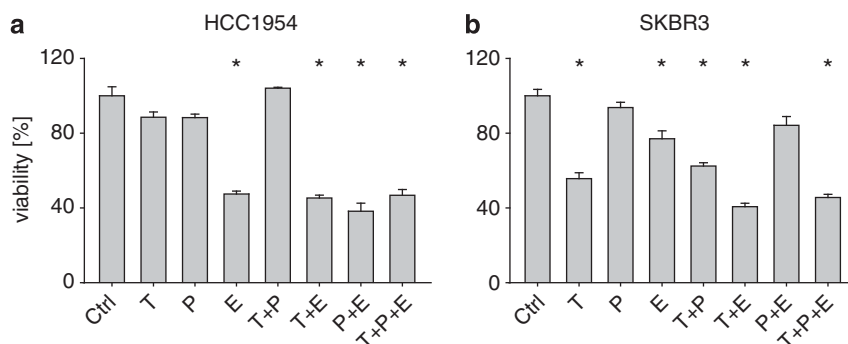


**Figure 1.** Impact of targeted therapeutics on cell viability. Cell viability was assessed after 96 h using the CellTiter-Blue assay. HCC1954 (a) and SKBR3 (b) cells were cultivated under the standard growth conditions and exposed to single drugs separately (trastuzumab, pertuzumab and erlotinib), as well as to all possible combinations. Erlotinib alone reduced HCC1954 cell viability, whereas in SKBR3 cells, effects mediated by trastuzumab and erlotinib were additive. Bar plots represent the means of four replicates. Significant differences are indicated with asterisks ( $P < 0.01$ ). Supplementary Figure S2 shows the impact of drug on cell viability after 24, 48, 72 and 96 h for both cell lines.

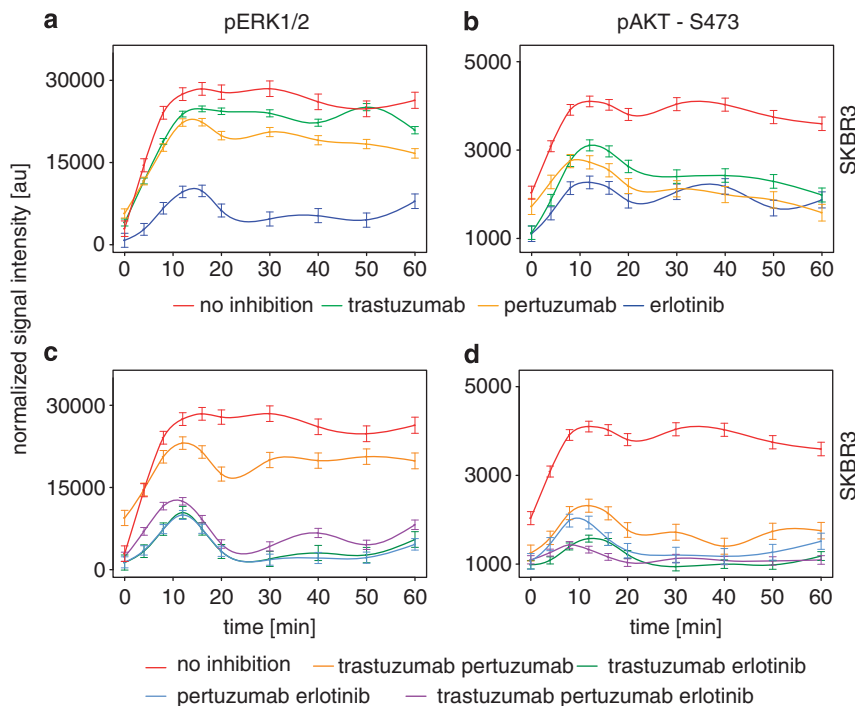


**Figure 2.** Impact of therapeutics on EGF-induced fast signaling. Data show EGF-induced ERK1/2 (a and c) and AKT (b and d) phosphorylation after preincubation of SKBR3 cells with trastuzumab, pertuzumab or erlotinib (a and b), as well as with all possible combinations (c and d). Phosphorylation dynamics were analyzed by RPPA. EGF (5 nM) induced phosphorylation of AKT and ERK1/2 in serum-starved SKBR3 cells. Pertuzumab and trastuzumab downregulated AKT signaling, whereas erlotinib, applied alone and in all combinations with therapeutic antibodies, inhibited the activation of both the pathways. Corresponding data set for HCC1954 cells is shown as Supplementary Figure S3 and Supplementary Table S1.

regarding the impact of both therapeutic antibodies on EGF-induced AKT signaling disappeared 30–60 min after adding EGF (Figure 2b). In summary, trastuzumab as well as pertuzumab revealed a strong inhibitory impact on EGF-induced AKT signaling in SKBR3 cells (Figures 2b and d) but did not prevent a concomitant activation of ERK1/2 signaling (Figures 2a and c).

EGF-stimulation of PI3K-mutated HCC1954 cells resulted in steadily fluctuating levels of phosphorylated AKT, which was independent of the EGF concentration applied (data not shown), and persisted also after preincubation with trastuzumab, pertuzumab or both therapeutic antibodies (Supplementary Figures S3B and D). Trastuzumab- and pertuzumab-mediated effects on EGF-induced ERK1/2 signaling were also minor in HCC1954 cells (Supplementary Figures S3A and C).

Erlotinib revealed a strong impact on cellular signaling in model cell lines of EGFR-high/ERBB2-positive breast cancer

Preincubation of SKBR3 cells with erlotinib reduced the EGF-inducible maximum of phosphorylated ERK1/2 by 60–70%, and a full downregulation of ERK1/2 activation was observed 20 min after stimulation with EGF (Figure 2a). In addition, ERK1/2 and AKT signaling were both reduced after exposure of SKBR3 cells to erlotinib-containing drug combinations (Figures 2c and d and Table 1). In HCC1954 cells, erlotinib effectively reduced the baseline level of ERK1/2 phosphorylation and also the response to EGF but did not influence the characteristic fluctuation seen for phosphorylated AKT (Supplementary Figures S3A and B).

Heregulin-beta 1 (HRG)-induced signaling requires participation of EGFR in SKBR3 cells

To assess how an activation of ERBB3-mediated signals might influence drug efficacy, SKBR3 cells were stimulated with HRG. The addition of HRG triggered a two-fold stronger activation of AKT

**Table 1.** Drug impact on EGF-induced fast signaling in SKBR3 cells (% AU)

	0 min		12 min EGF		30 min EGF	
	pERK	pAKT	pERK	pAKT	pERK	pAKT
Control	6.6	34.3	87.5	97.2	100.0	98.8
E	0	6.2	30.9	39.5	14.6	35.7
T	10.8	7.2	82.0	68.3	77.8	46.4
P	16.5	25.0	71.3	52.5	66.3	38.2
ET	1.1	2.5	35.0	19.8	2.6	0
EP	0.6	5.1	32.8	31.3	1.9	8.6
TP	26.8	11.2	66.3	42.1	59.7	26.0
TPE	4.6	5.2	42.3	10.6	11.2	6.2

Abbreviations: EGF, epidermal growth factor; E, erlotinib; EP, erlotinib + pertuzumab; ET, erlotinib + trastuzumab; P, pertuzumab; T, trastuzumab; TP, trastuzumab + pertuzumab; TPE, trastuzumab + pertuzumab + erlotinib. Impact of E, T, P and combinatorial drug treatments (ET, EP, TP and TPE) on fast signaling in SKBR3 cells (Figure 2). The median of normalized triplicate measurements was used to calculate the impact of drug on cellular signaling. Scales ranging 0–100% were generated target protein-specific. Maximal readings of normalized fluorescent intensities of a certain time course were set to equal 100% and the minimum was set to equal 0%.

signaling when compared with adding equimolar amounts of EGF (Supplementary Figure S4), which is in line with a predominant formation of ERBB2/ERBB3 heterodimers in response to HRG. None of the antibody drugs abolished HRG-induced AKT signaling when added as a single compound (Supplementary Table S2). However, drug combinations comprising pertuzumab were more effective than those including trastuzumab. In detail, pretreatment of SKBR3 cells with pertuzumab and erlotinib strongly reduced the HRG-induced activation of AKT signaling by 60%, and a comparable efficiency was also obtained after preincubation with

the triple drug combination (Figure 3, Supplementary Table S2). The two other binary drug combinations, trastuzumab plus pertuzumab and trastuzumab plus erlotinib, reduced HRG-induced AKT signaling by 20% and 35%, respectively (Figure 3). Both antibody drugs did not abolish HRG-induced ERK1/2

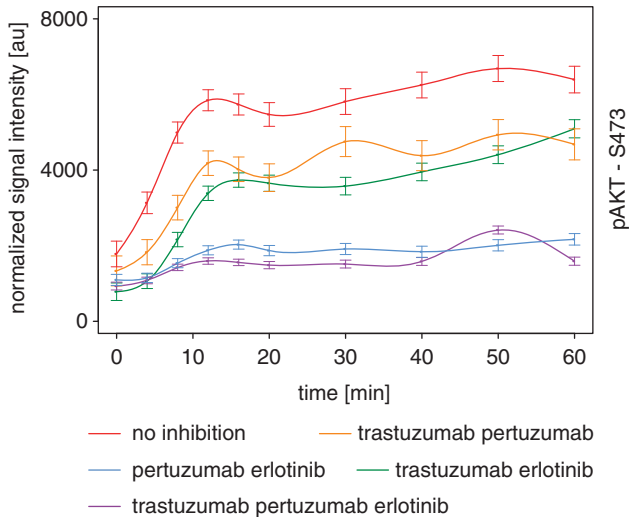


**Figure 3.** Impact of therapeutics on HRG-induced AKT signaling. Data show HRG-induced AKT phosphorylation after preincubation of SKBR3 cells with trastuzumab, pertuzumab or erlotinib for all possible combinations. Phosphorylation dynamics was analyzed by RPPA. HRG (5 nM) induced a phosphorylation of AKT signaling in serum-starved SKBR3 cells. Drug combinations downregulated HRG-induced AKT signaling, single drugs were ineffective. Corresponding data set for pERK1/2 dynamics is shown as Supplementary Figure S5. HCC1954 cells do not strongly respond to the addition of HRG due to low level ERBB3 expression (data not shown).

signaling when added alone or in combination (Supplementary Figure S5A), which was only seen after pretreatments including erlotinib (Supplementary Figure S5B). To sum up, only pertuzumab and erlotinib, but neither pertuzumab alone nor trastuzumab plus erlotinib, prevented the activation of AKT signaling in response to HRG in ERBB3-positive SKBR3 cells.

Phosphorylation states of RPS6 and RB reflect the impact of targeted therapeutics on ligand-induced signaling

Long-term impact of drug on the signaling pathways reflecting protein synthesis and cell-cycle progression was assessed by monitoring the dynamics of RPS6 (S235/S236) and RB (S807/S811) phosphorylation. Generally, a downregulation of RPS6 phosphorylation was seen after 8–10 h of drug exposure, whereas the impact of drug on RB phosphorylation became visible after 20–24 h (Figure 4).

Erlotinib alone as well as all erlotinib-containing drug combinations significantly reduced RPS6 and RB phosphorylation levels in HCC1954 cells (Figures 4a and c). On the contrary, preincubation of HCC1954 cells with a combination of trastuzumab and pertuzumab increased the phosphorylation rate of both proteins by two-fold (Figures 4a and c and Table 2). Additionally, c-MET phosphorylation increased after cotreatment of HCC1954 cells with trastuzumab and pertuzumab, indicating that after blocking ERBB2 signaling via c-MET gains importance (Figure 5). On the other hand, a combined treatment of SKBR3 cells with trastuzumab and erlotinib resulted in a fast and long-lasting dephosphorylation of RB and RPS6 (Figures 4b and d).

Taken together, in HCC1954 cells, erlotinib alone could efficiently reduce the phosphorylation rates of RB and RPS6. A benefit resulting from combination treatment was seen in SKBR3 cells after preincubation with trastuzumab and erlotinib. In summary, treatments reducing the viability of SKBR3 or HCC1954 cells after 96 h were identical with those that revealed a strong impact on cellular signaling.

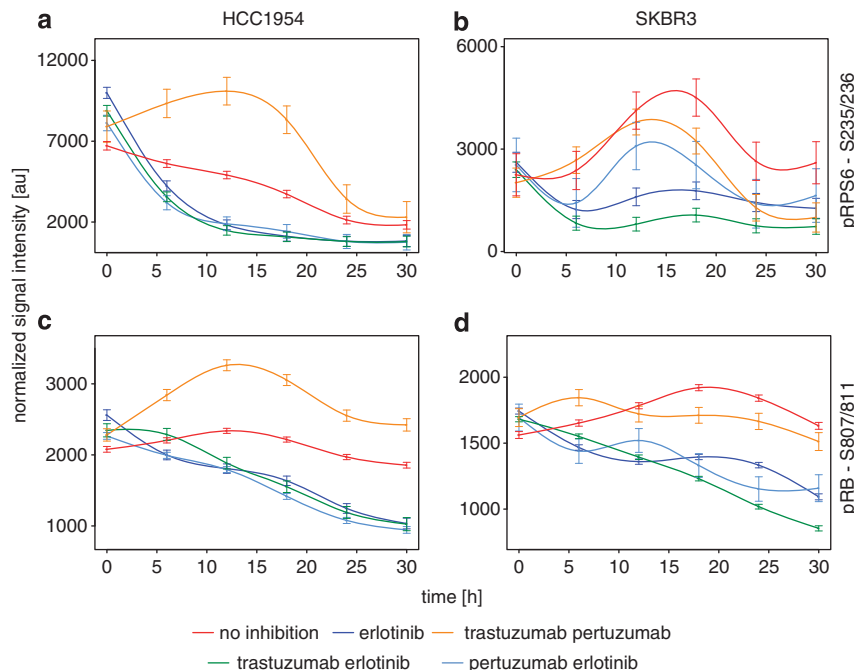


**Figure 4.** Long-term effects of targeted therapeutics on RPS6 and RB phosphorylation. Cells were exposed to erlotinib, pertuzumab/trastuzumab, trastuzumab/erlotinib or pertuzumab/erlotinib under standard growth conditions. Changes of protein phosphorylation were monitored over a time period of 30 h and analyzed by RPPA. Data show RPS6 (a and b) and RB (c and d) phosphoprotein dynamics in HCC1954 cells (a and c) and SKBR3 cells (b and d). Erlotinib and erlotinib-containing combinations downregulated RPS6 and RB phosphorylation of HCC1954 and SKBR3 cells.



**Table 2.** Impact of erlotinib (E) and combinatorial treatments (ET, EP, TP, TPE) on long-term signaling in SKBR3 cells and HCC1954 cells (Figure 4)

Cell line	SKBR3				HCC1954			
	pRPS6		pRB		pRPS6		pRB	
Hours	12	24	12	24	12	24	12	24
Control	64.6	28.6	87.0	93.7	43.8	12.6	59.9	42.2
E	19.5	13.0	46.9	46.6	12.4	0.7	36.4	10.6
ET	3.1	0	50.4	14.3	8.5	0.4	37.3	8.6
EP	53.4	10.4	70.0	26.8	14.1	0	37.1	4.4
TP	59.0	5.7	78.2	77.7	96.5	20.5	100.0	65.3
TPE	12.5	0.1	74.7	57.6	21.2	3.9	51.2	18.2

Abbreviations: E, erlotinib; EP, erlotinib + pertuzumab; ET, erlotinib + trastuzumab; P, pertuzumab; T, trastuzumab; TP, trastuzumab + pertuzumab; TPE, trastuzumab + pertuzumab + erlotinib. Scales ranging 0–100% were generated target protein-specific. Maximal readings of normalized fluorescent intensities of a certain time course were set to equal 100% and the minimum was set to equal 0%.

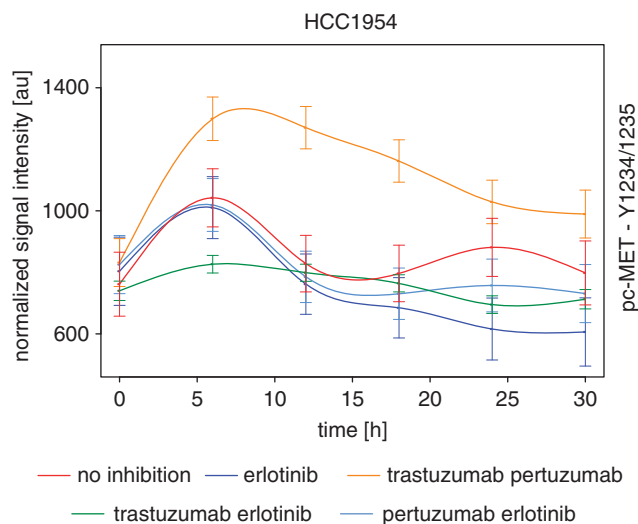


**Figure 5.** Long-term effects of targeted therapeutics on c-MET phosphorylation. Cells were exposed to drugs under the standard growth conditions. Changes of protein phosphorylation were monitored over a time period of 30 h and analyzed by RPPA. Data show c-MET phosphoprotein dynamics in HCC1954 cells. Cotreatment with trastuzumab and pertuzumab causes an increase of c-MET phosphorylation on Y1234/1235.

#### Immunohistochemical characterization of ERBB2-positive breast cancer specimens

To evaluate the clinical relevance of data obtained in cell line models of EGFR-high/ERBB2-amplified breast cancer, an immunohistochemical characterization was carried out for breast cancer specimens identified as HER2-amplified tumors in the clinic routine. In detail, the abundance of ERBB2, EGFR, estrogen and progesterone receptor was determined in 48 clinical specimens. Immunohistochemical data indicated that approximately one-third<sup>15</sup> of ERBB2-positive breast tumors coexpressed EGFR (Table 3). None of these tumors showed any detectable hormone-receptor expression, which was seen in another third of ERBB2-positive breast tumors<sup>14</sup> (Figures 6a and b and Table 3). A total of 19 tumors were positive for ERBB2 but for none of the other receptors (Figure 6c and Table 3). Moreover, the analysis of clinical data revealed that an increased number of patients with ERBB2-positive tumors that coexpress EGFR suffers from lymph

**Table 3.** Expression of EGFR, ERBB2, estrogen and progesterone receptors in human breast cancers identified as ERBB2-positive by immunohistochemistry

	Breast cancer subtypes		
	EGFR/ERBB2	ERBB2	Triple pos.
Total number	15	19	14
Relative number	31%	40%	29%
Age (years)	61.0	58.0	66.0
<i>Number of lymph node metastasis</i>			
0	3	13	7
1	8	4	6
2	3	0	0
3	1	2	1
Lymph node metastasis negative tumors	3	13	7
Lymph node metastasis positive tumors	12	6	7

Patients with breast cancers of the EGFR-high/ERBB2-positive subtype suffer more frequently of lymph node metastasis ( $P = 0.0129$ ).

node metastasis (12/15) in comparison with patients whose tumors expressed ERBB2 only (6/19) or patients with triple-positive tumors (7/14) (Table 3).

#### DISCUSSION

Signal propagation through ERBB receptors depends on receptor homo- or heterodimerization, which occurs mostly in response to ligand binding. ERBB2 presents the preferred binding partner as it does not require ligand activation for dimerization. Tumors express different subsets and levels of receptors and ligands, and for this reason, ERBB-mediated signaling depends on the protein repertoire of a particular tumor.<sup>33,34</sup> The rationale of current state-of-the-art treatment concepts employing both therapeutic antibodies is based on the strong impact that pertuzumab has on ligand-dependent signaling and the inhibition of ligand-independent ERBB2-mediated signaling by trastuzumab.<sup>17</sup> Clinical data indeed revealed a benefit rate of 50% by combination treatment for patients whose ERBB2-positive breast cancer had progressed under trastuzumab treatment.<sup>16,39,40</sup> However, still not all patients respond to the binary anti-ERBB2 treatment consisting of two different anti-ERBB2 antibodies. Thus, biomarker candidates need to be identified that are suitable for patient stratification ahead of treatment decisions.

In principle, high-level expression of two prominent proto-oncogenic growth-factor receptors might independently drive tumor progression, thus challenging treatment concepts that focus exclusively on the inhibition of ERBB2. Therefore, this study addressed the question, whether targeting ERBB2 is also sufficient to block tumor growth in EGFR-high/ERBB2-amplified breast cancer. Along these lines, the potential benefit of applying the EGFR-targeting small-molecule erlotinib in combination with trastuzumab or pertuzumab was assessed *in vitro* to obtain evidence for the design of future clinical trials targeting specifically EGFR in ERBB2-positive breast cancer. Substantial evidence for the existence of a separate ERBB2-amplified breast cancer subtype with high-level expression of activated EGFR has been demonstrated<sup>24</sup> and was evaluated in this study by analyzing data of an independent set of ERBB2-positive breast cancer patients. Furthermore, our data confirmed that the percentage of lymph-node-positive tumors is higher for ERBB2-positive breast cancer with high-level EGFR expression compared with tumors expressing ERBB2 only or triple-positive breast cancer.

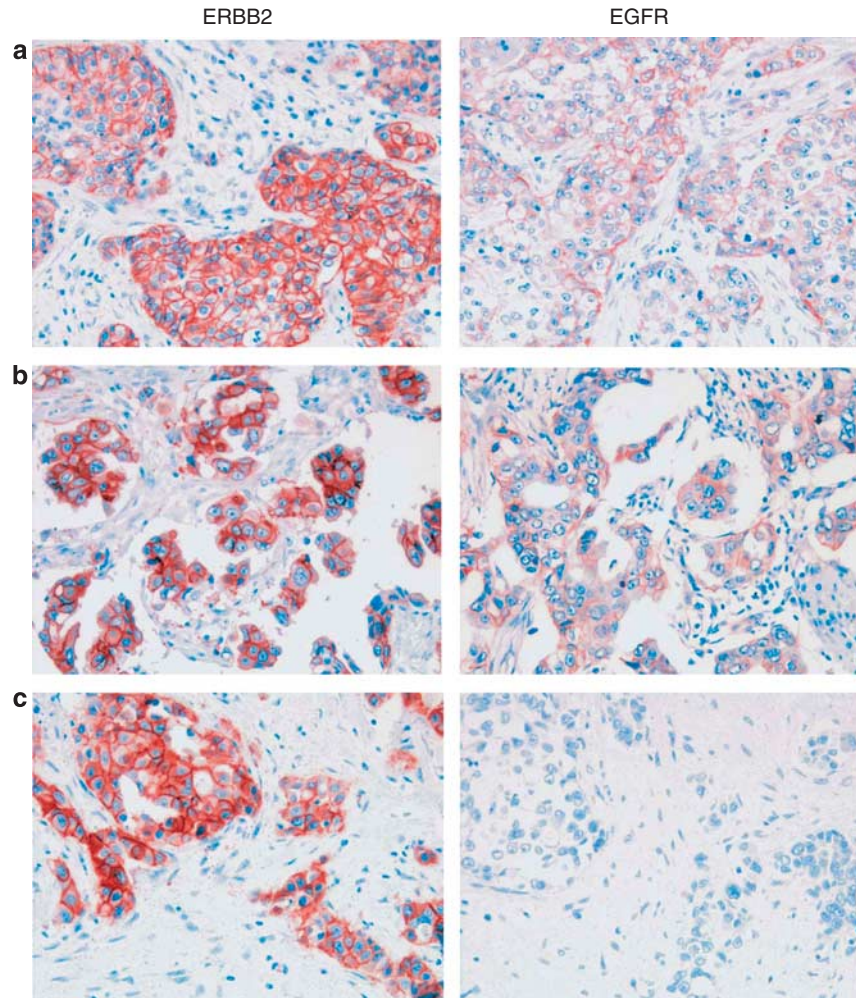


**Figure 6.** Selected clinical specimens illustrate ERBB2-amplified breast cancer as a heterogenous disease. Immunohistochemical detection of ERBB2 (left column) and EGFR (right column), magnification  $\times 200$ . EGFR-high/ERBB2-positive breast cancer (**a** and **b**) and ERBB2-amplified breast cancer without positive staining of EGFR (**c**).

Data obtained in this study showed on a mechanistic level that a combination of EGFR and ERBB2-targeting drugs produces a strong downregulation of signaling in EGFR-high/ERBB2-positive breast cancer cell lines.

The present data confirm that the EGF-induced activation of AKT signaling via EGFR/ERBB2 heterodimers is indeed amenable to inhibition by pertuzumab and trastuzumab combination treatment. Trastuzumab inhibits AKT-mediated signaling due to an abrogation of ligand-independent signaling, whereas pertuzumab prevents ligand-induced signaling, which is well in line with other reports.<sup>14,15</sup> However, ERK1/2 signaling was not affected as signal propagation via the ERK1/2 pathway can obviously be initiated by EGFR homodimers in an ERBB2-independent manner. This finding is in line with a previous report that demonstrated a shift of the ERBB-receptor dimer equilibrium towards increased numbers of EGFR homodimers after targeted inhibition of ERBB2.<sup>41</sup> The fact that erlotinib in combination with trastuzumab or pertuzumab can completely abolish EGF-induced signaling in SKBR3 cells suggests that both receptors need to be fully inhibited to avoid activation of an EGFR-based bypass mechanism.

Major differences regarding the mode of action of the two therapeutic antibodies became evident when signaling in SKBR3 cells was triggered with HRG instead of EGF. HRG has been reported to induce the formation of HRG:ERBB3/ERBB2 receptor complexes, thus strongly activating AKT signaling.<sup>33,34</sup> Data obtained in SKBR3 cells demonstrate that pertuzumab alone was

not sufficient to block HRG-activated AKT signaling. However, HRG-induced activation of AKT signaling was fully inhibited when pertuzumab was applied in combination with erlotinib, whereas a combination of trastuzumab and erlotinib was less efficient. This indicates that EGFR/ERBB3 dimers contribute to a sustained activation of AKT signaling in response to HRG. The finding that EGFR needs to be coinhibited in addition to ERBB2/3 to prevent HRG-induced signaling points to a central role of EGFR for the propagation of HRG-induced signals in SKBR3 cells. Furthermore, a strong downregulation of RPS6 phosphorylation was seen after cotreatment of SKBR3 cells with trastuzumab and erlotinib, confirming data on a combinatorial use comprising the dual kinase inhibitor lapatinib and trastuzumab in ERBB2-amplified gastric cancer cells.<sup>42</sup>

The impact of trastuzumab and pertuzumab on downstream signaling was highly different in HCC1954 cells harboring the H1047R PI3K gain-of-function mutation. First of all, AKT phosphorylation dynamics observed in this cell line did not depend on ligand binding and was also not influenced by anti-ERBB2 drugs. Furthermore, combinatorial treatment of HCC1954 cells with trastuzumab and pertuzumab increased RPS6 and RB phosphorylation levels and activated c-MET, which can independently contribute to downstream signaling. Expression of c-MET, detected only in HCC1954 but not SKBR3 cells, has previously been associated with trastuzumab resistance.<sup>43</sup> Data obtained in this study indicated also that exposure of HCC1954 cells to

erlotinib resulted in a significant decrease of RPS6 and RB phosphorylation. Erlotinib, applied alone and in combination with other therapeutic antibodies, also revealed a rather strong impact on cell viability contrasting the concept of 'oncogene addiction'. This observation implies that oncogenic aberrations accumulated at later stages during tumor development can potentially overrun the function of early driver mutations so that early genomic aberrations may be carried on as passenger mutations. Drug resistance of SKBR3 cells strongly depends on the particular type of ligand, which reflects the fact that this cell line can use other receptors, for example, EGFR or ERBB3, to bypass a block of ERBB2. Cellular signaling circuits are decoupled from receptor-mediated signaling in PI3K-mutated HCC1954 cells, and inhibition of HCC1954 cells with anti-ERBB2 antibodies did therefore not present an efficient strategy. A retrospective analysis of a cohort of trastuzumab-treated breast cancer patients revealed that disease progress was faster in patients with ERBB2-positive tumors and mutated PI3K.<sup>44</sup>

Different molecular mechanisms might produce a certain 'drug-resistant' phenotype. Thus, unraveling drug-resistance mechanisms on a molecular level will result in a level of understanding that allows drafting of new treatment concepts for further clinical validation. The data presented here suggest that EGFR activation and thereby the activation of downstream signaling cascades can only be prevented by combined inhibition of ERBB2 and EGFR in ERBB2-positive breast cancer with high-level expression of EGFR. On the other hand, ERBB2-amplified and PI3K-mutated tumors will potentially present a phenotype resistant towards anti-ERBB2 drugs. In conclusion, it might be worthwhile to assess EGFR expression levels as well as the mutational status of PI3K in breast cancer specimens to improve treatment concepts for ERBB2-positive breast cancer.

## MATERIALS AND METHODS

### Cell culture

SKBR3 (HTB-30) cells were obtained from the ATCC (LGC Standards, Wesel, Germany) and cultivated in Dulbecco's Modified Eagles Medium supplemented with 10% fetal bovine serum and  $1 \times$  NEAA (GIBCO, Darmstadt, Germany). The cells were split two times per week. For stimulation experiments,  $4 \times 10^5$  cells were seeded in six-well plates, cultivated for 24 h and serum-starved for additional 24 h. The human breast cancer cell line HCC1954 (CRL-2338) was cultivated as recommended by ATCC. The cells were split three times per week. For stimulation experiments,  $2 \times 10^5$  cells were seeded in six-well plates and cultivated as described before. Each cell line was confirmed as authentic by cytogenetic analysis carried out at the DSMZ ([www.dsmz.de](http://www.dsmz.de)).

### Viability assay

Cells were seeded (HCC1954: 2500 cells per well; SKBR3: 5000 cells per well) in full growth medium in black F96 MicroWell plates (Nunc, Langensfeld, Germany) to result in four replicate measurements. After 24 h, targeted therapeutics trastuzumab (10 ng/ml), pertuzumab (10 ng/ml) and erlotinib (1  $\mu$ M) (Roche Diagnostics GmbH, Penzberg, Germany) were added alone or in combination and incubated for further 24, 48, 72 or 96 h. CellTiter-Blue reagent (Promega, Mannheim, Germany) was added according to the manufacturer's protocol and incubated for 3 h at 37 °C before measuring fluorescence using a Tecan Infinite 200 (Tecan, Crailsheim, Germany). To determine significant differences, student's *t*-tests were conducted and *P*-values were Bonferroni-corrected for multiple testing.

### Dynamic measurements

In short-term experiments, trastuzumab (10 ng/ $\mu$ l), pertuzumab (10 ng/ $\mu$ l) and erlotinib (1  $\mu$ M) (Roche Diagnostics GmbH, Penzberg, Germany) were added to cells in starvation medium either alone or in combinations 1 h prior to growth-factor stimulation. Cells were stimulated with 5 nM EGF (Sigma, Munich, Germany) or HRG (Labvision, Dreieich, Germany). Lysates were prepared after 0, 4, 8, 12, 16, 20, 30, 40, 50 and 60 min. Each experiment involving inhibition with targeted drugs was performed in three biological replicates, whereas measurements without inhibitors were

performed in five replicates. Short-term measurements were generated using an automated liquid handling system (Biomek FX; Beckman Coulter, Krefeld, Germany). Long-term signaling experiments were carried out in full growth medium to avoid confounding effects that are potentially caused by nutrient deficiency. Cells were incubated in the standard medium for 24 h before addition of trastuzumab, pertuzumab and erlotinib in the same concentrations as above. Therapeutics were applied either alone (erlotinib) or in combination and cells were lysed after 0, 6, 12, 18, 24 and 30 h. Long-term measurements were carried out manually.

### Cell lysis and sample preparation

Medium was replaced by ice-cold phosphate-buffered saline, plates were transferred on ice and cells were harvested manually by scraping in M-PER lysis buffer (Pierce, Bonn, Germany) containing protease inhibitor Complete Mini and phosphatase inhibitor PhosSTOP (Roche, Mannheim, Germany). Cells were lysed for 20 min on an end-over-end shaker and lysates were cleared at by centrifugation at 16 000 g.

### Antibody characterization

Antibodies were analyzed for specificity by western blot analysis, and only highly specific antibodies were used for RPPA analysis. Dilution series of protein lysates were included in each printing run to confirm a linear correlation between protein concentration and antibody signal. Protein lysates were prepared from HCC1954 and SKBR3 cells cultured in the standard medium or stimulated with EGF or HRG for 12 min after starvation. The following antibodies were used for western blot and RPPA analysis: AKT (sc-1619-R; Santa Cruz Biotechnology, Santa Cruz, CA, USA), ERK1/2 (06-182; Millipore, Billerica, MA, USA), pAKT (S475, 9271), pERK1/2 (T202/Y204, 4370), EGFR (2646), RPS6 (2217), pRPS6 (S235/236, 4858), pRB (S807/811, 9308), c-MET (3148) and pc-MET (Y1234/1235, 3129) (Cell Signaling Technologies, Beverly, MA, USA), ERBB2 (Ab-17) and ERBB3 (Ab-2) were from Neomarkers (Fremont, CA, USA).

### Western blot analysis

Western blot analysis was carried out by loading 20  $\mu$ g total protein lysate per well in SDS-PAGE. The polyvinylidene difluoride membrane was blocked in 50% blocking buffer for near-infrared fluorescent western blotting (Rockland, Gilbertsville, PA, USA) in Tris-buffered saline containing 5 mM sodium fluoride and 1 mM sodium vanadate. Primary antibodies were diluted 1:1000 in blocking buffer and incubated overnight. Secondary Alexa 680-labeled antibodies (Molecular Probes, Darmstadt, Germany) were diluted 1:10 000 in Tris-buffered saline Tween-20. Blots were scanned on the Odyssey Infrared Imaging System (LI-COR, Lincoln, NE, USA).

### Quantitative reverse transcription PCR

Quantitative reverse transcription PCR was performed using Taqman Gene Expression Assays (Applied Biosystems, Darmstadt, Germany) for EGFR (Hs00193306\_m1), ERBB2 (Hs00170433\_m1), ERBB3 (Hs00176538\_m1), ERBB4 (Hs00171783\_m1), c-MET (Hs00179845\_m1) and GAPDH (Hs99999905\_m1). RNA was isolated using the RNeasy Kit according to the manufacturer's protocol (Qiagen, Hilden, Germany). First strand synthesis of cDNA was carried out using the ReverdAid H-Minus First Strand cDNA Synthesis Kit (Fermentas, St. Leon-Rot, Germany). The quantitative reverse transcription PCR reaction was executed using a 7900HT Fast Real-Time PCR System. The assay was preheated for 2 min at 50 °C and 15 min at 95 °C. The reaction cycle of 15 s/95 °C and 1 min/60 °C was repeated 40 times. PCR reactions were performed in triplicate. Samples were normalized for GAPDH expression and adjusted to receptor expression levels of MCF7 cells using the R-package 'ddCT'.<sup>45</sup>

### Processing of RPPAs

Total protein concentration was determined using the bicinchoninic acid (BCA) method (Pierce). Lysates were adjusted to a total protein concentration between 1.2 and 3  $\mu$ g/ $\mu$ l. Prior to printing, samples were mixed with Tween-20 to result in a final concentration of 0.05%. The samples were printed in triplicate onto nitrocellulose-coated glass slides (Oncyte; Grace-Biolabs, Bend, OR, USA) using a contact spotter (2470 Arrayer; Aushon Biosystems, Billerica, MA, USA) equipped with 180  $\mu$ m pins. Slides were blocked in 50% Odyssey blocking buffer (LI-COR) in phosphate-buffered saline containing 5 mM sodium fluoride and 1 mM sodium vanadate. Primary antibodies were diluted 1:300 in antibody diluent with background reducing components (Dako, Glostrup, Denmark). Alexa 680-



labeled secondary antibodies (Molecular Probes) were diluted 1:8000. After drying, slides were scanned on the Odyssey Infrared Imaging System (LI-COR). A single slide was used for total protein quantification per spotting run after staining with Fast Green FCF staining buffer (Sigma, Steinheim, Germany) as described before.<sup>35</sup>

#### RPPA data analysis

Signal intensities were determined using the GenePix Pro5.0 software (Molecular Devices, Sunnyvale, CA, USA) resulting in gpr files. Data analysis was carried out using the statistical software environment R.<sup>46</sup> For further analysis, raw data was normalized by calculating spot-specific correction factors based on signal intensities of the FCF slide and correcting the readout of slides probed with antibodies.<sup>35</sup> The median of biological and technical replicates was calculated for a certain treatment and for each time point. This data set was used to calculate smoothing splines for each phosphoprotein. Spline calculation started with a constant model fit, and degrees of freedom were increased stepwise resulting in more complex model fits. All model fits representing increasing degrees of freedom were compared with the constant model fit using analysis of variance at a significance level of 5%. The model fit with the smallest *P*-value was chosen for the graphic presentation of dynamic data. Error bars were calculated as point wise s.e. of the spline fit representing the noise of biological replicates. To compare two experimental conditions, for example, no drug treatment vs erlotinib treatment, Welch two-sample *t*-tests were conducted to test whether the mean of biological replicates differed significantly between treatments. This analysis was performed in cell line- and target protein-specific manner. To describe treatment effects quantitatively, a minimum-maximum normalization was applied to define a scale ranging between 0 and 1 based on median signal intensities.<sup>47</sup> The maximum reading of 1 was considered to correspond to 100% of phosphorylation observed for a certain series of experiments. Microarray data are available via the GEO accession number GSE36327.<sup>48,49</sup>

#### Tumor samples and immunohistochemistry

Tissue microarrays containing a total of 50 ERBB2-overexpressing primary breast carcinomas were collected from the Institute of Pathology of Heidelberg University Clinics and Tissue Bank of the National Center for Tumor Diseases. ERBB2 status had previously been assessed immunohistochemically using a polyclonal antiserum (1:500, A0485; DakoCytomation, Hamburg, Germany). In three cases with equivocal (score 2+) staining results, HER2 positivity had been verified by fluorescence *in situ* hybridization. EGFR immunostaining was carried out with a mouse anti-human monoclonal antibody (31G5; Zytomed, Berlin, Germany) at a dilution of 1:25 following Pronase E pretreatment (0.1% w/v in phosphate-buffered saline, 6 min at 37 °C). Visualization was performed using the Chemmate peroxidase/AEC-Kit (avidin-biotin-complex method; DakoCytomation) according to the manufacturer's instructions.

#### CONFLICT OF INTEREST

MH is an employee of Roche Diagnostics GmbH, Penzberg, Germany. The remaining authors declare no conflict of interest.

#### ACKNOWLEDGEMENTS

We are grateful for the skillful technical assistance of Corinna Becki, Maike Wosch and Sabrina Schumacher. Pertuzumab, trastuzumab and erlotinib were provided by Roche Diagnostics GmbH, Penzberg, Germany. This work was supported within the National Genome Research Network (grant 01G50864) and the Medical Systems Biology program (grant 0315396B) of the German Federal Ministry of Education and Research (BMBF).

#### REFERENCES

- Slamon DJ, Clark GM, Wong SG, Levin WJ, Ullrich A, McGuire WL. Human breast cancer: correlation of relapse and survival with amplification of the HER-2/neu oncogene. *Science* 1987; **235**: 177–182.
- Tzahar E, Waterman H, Chen X, Levkowitz G, Karunagaran D, Lavi S et al. A hierarchical network of interreceptor interactions determines signal transduction by Neu differentiation factor/neuregulin and epidermal growth factor. *Mol Cell Biol* 1996; **16**: 5276–5287.
- Hendriks BS, Opreko LK, Wiley HS, Lauffenburger D. Coregulation of epidermal growth factor receptor/human epidermal growth factor receptor 2 (HER2) levels and locations: quantitative analysis of HER2 overexpression effects. *Cancer Res* 2003; **63**: 1130–1137.
- Karunagaran D, Tzahar E, Beerli RR, Chen X, Graus-Porta D, Ratzkin BJ et al. ErbB-2 is a common auxiliary subunit of NDF and EGF receptors: implications for breast cancer. *EMBO J* 1996; **15**: 254–264.
- Sliwkowski MX, Schaefer G, Akita RW, Lofgren JA, Fitzpatrick VD, Nuijens A et al. Coexpression of erbB2 and erbB3 proteins reconstitutes a high affinity receptor for heregulin. *J Biol Chem* 1994; **269**: 14661–14665.
- Carter P, Presta L, Gorman CM, Ridgway JB, Henner D, Wong WL et al. Humanization of an anti-p185HER2 antibody for human cancer therapy. *Proc Natl Acad Sci USA* 1992; **89**: 4285–4289.
- Slamon DJ, Leyland-Jones B, Shak S, Fuchs H, Paton V, Bajamonde A et al. Use of chemotherapy plus a monoclonal antibody against HER2 for metastatic breast cancer that overexpresses HER2. *N Engl J Med* 2001; **344**: 783–792.
- Viani GA, Afonso SL, Stefano EJ, De Fendi LI, Soares FV. Adjuvant trastuzumab in the treatment of her-2-positive early breast cancer: a meta-analysis of published randomized trials. *BMC Cancer* 2007; **7**: 153.
- Clynes RA, Towers TL, Presta LG, Ravetch JV. Inhibitory Fc receptors modulate *in vivo* cytotoxicity against tumor targets. *Nat Med* 2000; **6**: 443–446.
- Molina MA, Codony-Servat J, Albanell J, Rojo F, Arribas J, Baselga J. Trastuzumab (herceptin), a humanized anti-Her2 receptor monoclonal antibody, inhibits basal and activated Her2 ectodomain cleavage in breast cancer cells. *Cancer Res* 2001; **61**: 4744–4749.
- Neve RM, Chin K, Fridlyand J, Yeh J, Baehner FL, Fevr T et al. A collection of breast cancer cell lines for the study of functionally distinct cancer subtypes. *Cancer Cell* 2006; **10**: 515–527.
- Izumi Y, Xu L, di Tomaso E, Fukumura D, Jain RK. Tumour biology: herceptin acts as an anti-angiogenic cocktail. *Nature* 2002; **416**: 279–280.
- Spector NL, Blackwell KL. Understanding the mechanisms behind trastuzumab therapy for human epidermal growth factor receptor 2-positive breast cancer. *J Clin Oncol* 2009; **27**: 5838–5847.
- Junttila TT, Akita RW, Parsons K, Fields C, Lewis PGD, Friedman LS et al. Ligand-independent HER2/HER3/PI3K complex is disrupted by trastuzumab and is effectively inhibited by the PI3K inhibitor GDC-0941. *Cancer Cell* 2009; **15**: 429–440.
- Franklin MC, Carey KD, Vajdos FF, Leahy DJ, de Vos AM, Sliwkowski MX. Insights into ErbB signaling from the structure of the ErbB2-pertuzumab complex. *Cancer Cell* 2004; **5**: 317–328.
- Scheuer W, Friess T, Burtscher H, Bossenmaier B, Endl J, Hasmann M. Strongly enhanced antitumor activity of trastuzumab and pertuzumab combination treatment on HER2-positive human xenograft tumor models. *Cancer Res* 2009; **69**: 9330–9336.
- Baselga J, Swain SM. Novel anticancer targets: revisiting ERBB2 and discovering ERBB3. *Nat Rev Cancer* 2009; **9**: 463–475.
- Baselga J, Cortes J, Kim SB, Im SA, Hegg R, Im YH et al. Pertuzumab plus trastuzumab plus docetaxel for metastatic breast cancer. *N Engl J Med* 2012; **366**: 109–119.
- O'Brien NA, Browne BC, Chow L, Wang Y, Ginther C, Arboleda J et al. Activated phosphoinositide 3-kinase/AKT signaling confers resistance to trastuzumab but not lapatinib. *Mol Cancer Ther* 2010; **9**: 1489–1502.
- Nagata Y, Lan KH, Zhou X, Tan M, Esteva FJ, Sahin AA et al. PTEN activation contributes to tumor inhibition by trastuzumab, and loss of PTEN predicts trastuzumab resistance in patients. *Cancer Cell* 2004; **6**: 117–127.
- Sahin O, Frohlich H, Lobke C, Korf U, Burmester S, Majety M et al. Modeling ERBB receptor-regulated G1/S transition to find novel targets for de novo trastuzumab resistance. *BMC Syst Biol* 2009; **3**: 1.
- Roberts PJ, Der CJ. Targeting the Raf-MEK-ERK mitogen-activated protein kinase cascade for the treatment of cancer. *Oncogene* 2007; **26**: 3291–3310.
- Hidalgo M. Erlotinib: preclinical investigations. *Oncology* 2003; **17**(Suppl 12): 11–16.
- Gonzalez-Angulo AM, Hennessy BT, Meric-Bernstam F, Sahin A, Liu W, Ju Z et al. Functional proteomics can define prognosis and predict pathologic complete response in patients with breast cancer. *Clin Proteomics* **8**: 11.
- Schneeweiss A, Kolay S, Aulmann S, Von Minckwitz G, Torode J, Koehler M et al. Induction of remission in a patient with metastatic breast cancer refractory to trastuzumab and chemotherapy following treatment with gefitinib ('Iressa', ZD1839). *Anticancer Drugs* 2004; **15**: 235–238.
- Olayioye MA, Neve RM, Lane HA, Hynes NE. The ErbB signaling network: receptor heterodimerization in development and cancer. *EMBO J* 2000; **19**: 3159–3167.
- Schulze WX, Deng L, Mann M. Phosphotyrosine interactome of the ErbB-receptor kinase family. *Mol Syst Biol* 2005; **1**: 2005 0008.
- Yarden Y, Sliwkowski MX. Untangling the ErbB signalling network. *Nat Rev Mol Cell Biol* 2001; **2**: 127–137.



- 29 Hellyer NJ, Kim MS, Koland JG. Heregulin-dependent activation of phosphoinositide 3-kinase and Akt via the ErbB2/ErbB3 co-receptor. *J Biol Chem* 2001; **276**: 42153–42161.
- 30 Jones RB, Gordus A, Krall JA, MacBeath G. A quantitative protein interaction network for the ErbB receptors using protein microarrays. *Nature* 2006; **439**: 168–174.
- 31 Manning BD. Balancing Akt with S6K: implications for both metabolic diseases and tumorigenesis. *J Cell Biol* 2004; **167**: 399–403.
- 32 Lane HA, Motoyama AB, Beuvink I, Hynes NE. Modulation of p27/Cdk2 complex formation through 4D5-mediated inhibition of HER2 receptor signaling. *Ann Oncol* 2001; **12**(Suppl 1): S21–S22.
- 33 Citri A, Yarden Y. EGF-ERBB signalling: towards the systems level. *Nat Rev Mol Cell Biol* 2006; **7**: 505–516.
- 34 Hynes NE, MacDonald G. ErbB receptors and signaling pathways in cancer. *Curr Opin Cell Biol* 2009; **21**: 177–184.
- 35 Loebke C, Sueltmann H, Schmidt C, Henjes F, Wiemann S, Poustka A *et al*. Infrared-based protein detection arrays for quantitative proteomics. *Proteomics* 2007; **7**: 558–564.
- 36 Niu G, Carter WB. Human epidermal growth factor receptor 2 regulates angiopoietin-2 expression in breast cancer via AKT and mitogen-activated protein kinase pathways. *Cancer Res* 2007; **67**: 1487–1493.
- 37 Chakrabarty A, Rexer BN, Wang SE, Cook RS, Engelman JA, Arteaga CL. H1047R phosphatidylinositol 3-kinase mutant enhances HER2-mediated transformation by heregulin production and activation of HER3. *Oncogene*. **29**: 5193–5203.
- 38 Nahta R, Yuan LX, Zhang B, Kobayashi R, Esteva FJ. Insulin-like growth factor-I receptor/human epidermal growth factor receptor 2 heterodimerization contributes to trastuzumab resistance of breast cancer cells. *Cancer Res* 2005; **65**: 11118–11128.
- 39 Baselga J, Gelmon KA, Verma S, Wardley A, Conte P, Miles D *et al*. Phase II trial of pertuzumab and trastuzumab in patients with human epidermal growth factor receptor 2-positive metastatic breast cancer that progressed during prior trastuzumab therapy. *J Clin Oncol*. **28**: 1138–1144.
- 40 Gianni L, Pienkowski T, Im YH, Roman L, LM T, Liu MC *et al*. Efficacy and safety of neoadjuvant pertuzumab and trastuzumab in women with locally advanced, inflammatory, or early HER2-positive breast cancer (NeoSphere): a randomised multicentre, open-label, phase 2 trial. *The Lancet* 2011; **11**: 70336–70339.
- 41 Hughes JB, Berger C, Rodland MS, Hasmann M, Stang E, Madhus IH. Pertuzumab increases epidermal growth factor receptor down-regulation by counteracting epidermal growth factor receptor-ErbB2 heterodimerization. *Mol Cancer Ther* 2009; **8**: 1885–1892.
- 42 Wainberg ZA, Anghel A, Desai AJ, Ayala R, Luo T, Safran B *et al*. Lapatinib, a dual EGFR and HER2 kinase inhibitor, selectively inhibits HER2-amplified human gastric cancer cells and is synergistic with trastuzumab *in vitro* and *in vivo*. *Clin Cancer Res* 2010; **16**: 1509–1519.
- 43 Shattuck DL, Miller JK, Carraway 3rd KL, Sweeney C. Met receptor contributes to trastuzumab resistance of Her2-overexpressing breast cancer cells. *Cancer Res* 2008; **68**: 1471–1477.
- 44 Razi E, Bobos M, Kotoula V, Eleftheraki AG, Kalofonos HP, Pavlakis K *et al*. Evaluation of the association of PIK3CA mutations and PTEN loss with efficacy of trastuzumab therapy in metastatic breast cancer. *Breast Cancer Res Treat. Jul* **128**: 447–456.
- 45 Chang S, Chen W, Yang J. Another formula for calculating the gene change rate in real-time RT-PCR. *Mol Biol Rep* 2009; **36**: 2165–2168.
- 46 R Development Core Team. *R: a language and environment for statistical computing*. R Foundation for Statistical Computing; Vienna, Austria, 2011.
- 47 Han J, Kamber M. *Data Mining: Concepts and Techniques*. 2nd edn (Morgan Kaufman: Waltham, MA, USA, 2000).
- 48 Edgar R, Domrachev M, Lash AE. Gene Expression Omnibus: NCBI gene expression and hybridization array data repository. *Nucl Acid Res* 2002; **30**: 207–210.
- 49 Barrett T, Troup DB, Wilhite SE, Ledoux P, Evangelista C, Kim IF *et al*. NCBI GEO: archive for functional genomics data sets—10 years on. *Nucl Acids Res* 2011; **39**: D1005–D1010.



*Oncogenesis* is an open-access journal published by Nature Publishing Group. This work is licensed under the Creative Commons Attribution-NonCommercial-No Derivative Works 3.0 Unported License. To view a copy of this license, visit <http://creativecommons.org/licenses/by-nc-nd/3.0/>

Supplementary Information accompanies the paper on the *Oncogenesis* website (<http://www.nature.com/oncsis>).